A DER based Voltage Control Strategy for Microgrids

Giovanni Massa
Vincenzo Galdi
Vito Calderaro
Antonio Piccolo
Department of Industrial Engineering
University of Salerno
Fisciano (SA), Italy
gv.massa@gmail.com, vgaldi@unisa.it

George Gross
Department of Electrical and Computer Engineering
University of Illinois at Urbana-Champaign
Urbana, Illinois, USA
gross@illinois.edu

***Abstract*—Recently, the ability of microgrids (μgs) to allow a deeper penetration of Distributed Energy Resources (DERs) in Distribution Networks (DNs) has facilitated their widely spread deployment. Because of the variability associated with the loads and the intrinsic intermittent and nature of renewable energy resources, the development and implementation of effective voltage control strategies is essential to reliably serve the loads, in particular when working islanded from the main grid. To face this problem, we propose a dispersed control approach capable to maintain voltage levels within the operational limits by means of DERs reactive and active power support. We implement an optimization framework to prove the robustness of the proposed control methodology. We illustrate the effectiveness of the proposed methodology with a set of representative studies from the testing of the simulation approach we performed, proving the absence of any opportunity cost involved by the control action.**

***Index Terms*—Distributed energy resources, microgrid, reactive power support, renewable energy sources, voltage control.**

I. Introduction

The integration of Distributed Energy Resources (DERs) connected at the Distribution Network (DN) level is representing a complication in network operations and control. On the other hand, the deployment of smart grid technologies provides the opportunity to develop new techniques to better address the issues related to the variability in the loads as well as the intrinsic intermittent nature of such resources [1]. In particular, the microgrid (μg) concept is emerging in recent years as a promising approach to optimally manage DNs with deep penetration of DERs.

According to its general structure, a μg could be defined as a group of interconnected DERs (generators, storage devices and controllable loads), which, together with imports, can meet the internal demand and the contracted exports, working either in the Grid Connected Mode (GCM) or the Islanded Operations Mode (IOM) with respect to the main grid. Thus, the DERs contained within the μg should be able to provide the various services required for its secure operations, such as the generation-demand balance and the provision of proper voltage control and reactive power support [2]. This work addresses the latter problem and presents an effective approach to face voltage control issues.

Previous works on voltage control strategies applied to DNs and μgs have been focused on centralized control strategies [3]-[5] and distributed/decentralized techniques [6]-[10]. In particular, distributed/decentralized control schemes use various resources, including Distributed Generators (DGs), Energy Storage Systems (ESSs) or Demand Response Resources (DRRs). These approaches prove how the utilization of DERs could guarantee a wider flexibility compared to traditional control schemes while facing the voltage control problem. The main lack of previous works is the utilization of only some of the DERs available within a μg to implement the voltage control actions and their application to only a single operations condition, looking at the GCM or at the IOM separately. Furthermore, they do not include the voltage control strategy into a cost-effective framework.

To overcome the presented limitations, we introduce a comprehensive utilization of the μg resources to face the voltage control problem. We explicitly address the voltage control issue through the formulation of local control strategies using DERs, in both the GCM and the IOM, modeling the control capability of the various resources. We perform the voltage control at the Point of Common Coupling (PCC) between the DER and the μg feeder. We provide the DER control action specifications through an optimization framework that incorporates all the physical and regulatory constraints, including the DER capability curves, the regulatory requirements, the power factor specifications, the network characteristics and the market environment. Under the GCM, the demand is met with the imports from the main grid, with cost minimization being the appropriate objective function. Under the IOM, the optimization is based on the DER production costs, in order to

The work has been conducted while G. Massa was with the Department of Industrial Engineering of the University of Salerno, during his cooperation with the University of Illinois at Urbana-Champaign.

meet at least the critical load requirements. Whenever the DER capacities are inadequate to satisfy the loads, the procedure makes use of DRRs to ensure the critical loads are served.

We show the effectiveness of the proposed approach with a set of representative studies from the testing of the simulation approach we performed. Simulation results show the capability of the proposed approach to present a cost effective solution that guarantees an economic operation for both the GCM and the IOM and to: a) avoid the DER disconnection from the grid due to the violation of the specified voltage limits; b) overcome the use of Volt/VAr devices that may face several challenges due to their interaction with DERs and may be inadequate to furnish the required functionalities during the IOM; c) guarantee critical loads served during the islanding condition; d) avoid the entailment of any opportunity cost involved by the required control action [11].

The paper has four additional sections. In Section II, we address the basic concepts of the proposed μg resources, introducing the proposed voltage control approach. We illustrate in Section III the snapshot optimization framework for both the μg operation modes. In Section IV, we provide representative results from the testing phase performed on the system under study, outlining concluding remarks in Section V.

II. Local Voltage Control Approach

The traditional devices used to control voltage levels and to furnish reactive power support in DNs include fixed or switched capacitor banks, step voltage regulators and on-load tap-changing transformers, which are not designed to handle the DERs variability and could face several limitations [12]. Thus, within this framework, we implement the voltage control action at the PCC between the DER and the μg feeder by making use of DERs reactive and/or active power output control capabilities.

A. DERs Control Capabilities in a Microgrid

We define the control capabilities of the μg resources as depicted in Table I, where symbols "+", "-", "±" describe the capability of the DER to act on the generated, absorbed, or both active (p) and reactive (q) power, respectively. We consider a general model in which the μg is equipped with the DERs described in the following.

We take into account that DGs, as well as ESSs (e.g. batteries), are often connected to the grid by means of Power Electronic Interfaces (PEIs). These interfaces allow the DG and the ESS to manage active/reactive power within the limits defined by the PEI capability curves and the resource actual power limits [9]. We model ESSs taking into account that they must accomplish a full cycle over the study period. We try to use the ESS economically, assuring that the marginal cost of the charging energy is less than the one displaced during the discharging phase [13]. Defining the charge-discharge cycle efficiency η_s given by the product between the ESS charging and discharging efficiencies (η_c, η_d), we obtain:

$$\eta_c \varepsilon_c = \frac{\varepsilon_d}{\eta_d} \Rightarrow \eta_s \varepsilon_c = \varepsilon_d \tag{1}$$

TABLE I. DERs Control Capabilities

<table>
<tr><th>DER type</th><th>DER interface</th><th colspan="2">Control</th></tr>
<tr><td>Fixed-speed wind turbines</td><td>Induction generator</td><td rowspan="6">+p</td><td>-q</td></tr>
<tr><td>Small hydro reciproc. engines</td><td>Synchronous generator</td><td rowspan="8">±q</td></tr>
<tr><td>Variable-speed wind turbines</td><td rowspan="7">PEI</td></tr>
<tr><td>Photovoltaic</td></tr>
<tr><td>Fuel cell</td></tr>
<tr><td>Microturbine</td></tr>
<tr><td>Flywheel</td><td rowspan="3">±p</td></tr>
<tr><td>Battery storage systems</td></tr>
<tr><td>Supercapacitor</td></tr>
<tr><td>Demand response resource</td><td>controlled switch</td><td>-p</td><td></td></tr>
</table>

where ε_c is the energy taken during the charging phase and ε_d the energy delivered to the load.

We take into account the potential impact of DRRs on voltage levels by means of variation of the active power absorbed by controllable loads. We integrate DRRs in the proposed approach taking into account the chronological limitations of typical demand response programs. In order to reduce the impact on customers, we use these resources as a lowest effectiveness variable to perform the proposed control action.

B. Sensitivity Factors Based Local Voltage Control

The voltage control methodology we define is based on the sensitivity of voltage levels to active and reactive power variations from DERs at the μg buses. We model the μg with N+1 buses and L lines. Thus, we indicate in (2) the set of buses $\mathscr{N}$ and the set of lines $\mathscr{L}$ connecting the buses in $\mathscr{N}$ by associating to each line $l \in \mathscr{L}$ the node pair (n,h) so that $l \leftrightarrow (n,h)$.

$$\begin{aligned} \mathscr{N} &= \{n : n = 0,1,2,...,N\} \\ \mathscr{L} &= \{l : l = 1,2,...,L\} \end{aligned} . \tag{2}$$

Bus 0 represents the external tie-line connecting the μg to the main grid. We consider the M PV buses with $M < N$ to be numbered from 1 to M, and buses M+1 to N constituting the N-M PQ buses. We change the amount M of PV buses depending on the μg configuration and the dispatched resources.

We represent the index set of DGs and DRRs as in (3) and we implement the voltage control action by using the resources in $\mathscr{S} \cup \mathscr{R}$, assuming that it is possible to connect a single μg bus $n \in \mathscr{N}$ to multiple resources of $\mathscr{S} \cup \mathscr{R}$:

$$\begin{aligned} \mathscr{S} &= \{s_i : i = 1,2,...,S\} \\ \mathscr{R} &= \{r_j : j = 1,2,...,R\} \end{aligned} . \tag{3}$$

To associate each resource in $\mathscr{S} \cup \mathscr{R}$ to the corresponding connection node $n \in \mathscr{N}$, we define a mapping function f capable to implement the resource mapping as in (4):

$$\begin{aligned} \mathscr{S} \mapsto \mathscr{N} &: s_i \in \mathscr{S} \to n \in \mathscr{N} \\ \mathscr{R} \mapsto \mathscr{N} &: r_j \in \mathscr{R} \to n \in \mathscr{N} \end{aligned} . \tag{4}$$

We define the analysis period set as $\mathscr{T} = \{t_k : k = 1, 2, ..., K\}$ and we denote the voltage amplitude and angles for a given time step $t_k \in \mathscr{T}$ as in the following:

$$\begin{aligned} \boldsymbol{v}[t_k] &\triangleq \left[v_1[t_k], v_2[t_k], ..., v_N[t_k]\right]^T \\ \boldsymbol{\vartheta}[t_k] &\triangleq \left[\vartheta_1[t_k], \vartheta_2[t_k], ..., \vartheta_N[t_k]\right]^T \end{aligned} . \tag{5}$$

We consider $v_0[t_k]$ and $\vartheta_0[t_k]$ associated to the external reference bus. We define the voltage control problem to maintain the voltage profile $v_n[t_k]$ at each bus $n \in \mathscr{N}$ as dictated by regulatory requirements for each time snapshot t_k:

$$v_n^m \le v_n[t_k] \le v_n^M \quad \forall n \in \mathscr{N}, \forall t_k \in \mathscr{T}. \tag{6}$$

We refer to the net active and reactive power injection at each node $n \in \mathscr{N}$ by $p_n[t_k]$ and $q_n[t_k]$, thus we obtain:

$$\begin{aligned} \boldsymbol{p}[t_k] &\triangleq \left[p_1[t_k], p_2[t_k], ..., p_N[t_k]\right]^T \\ \boldsymbol{q}[t_k] &\triangleq \left[q_1[t_k], q_2[t_k], ..., q_N[t_k]\right]^T \end{aligned} . \tag{7}$$

We assume the voltage $(\Delta v_n[t_k])$ and angle $(\Delta\vartheta_n[t_k])$ variations during the time interval $[t_{k-1}, t_k]$ represented by a total variation occurring at the snapshot instant t_k. We compute the variation in voltage magnitude and angle during two consecutive time steps respectively as $\Delta v_n[t_k] = v_n[t_k] - v_n[t_{k-1}]$ and $\Delta\vartheta_n[t_k] = \vartheta_n[t_k] - \vartheta_n[t_{k-1}]$. These variations are related to active and/or reactive power variations $\Delta p_n[t_k]$ and $\Delta q_n[t_k]$ by (8), representing the linearization of the power flow equations around the operating point at a given instant. Each submatrix $\boldsymbol{J}_{xy}[t_k]$ represented in (8) is obtained by the power flow equations linearization around the operating point:

$$\begin{bmatrix} \boldsymbol{J}_{p\vartheta}[t_k] & \boldsymbol{J}_{pv}[t_k] \\ \boldsymbol{J}_{q\vartheta}[t_k] & \boldsymbol{J}_{qv}[t_k] \end{bmatrix} \begin{bmatrix} \Delta\boldsymbol{\vartheta}[t_k] \\ \Delta\boldsymbol{v}[t_k] \end{bmatrix} = \begin{bmatrix} \Delta\boldsymbol{p}[t_k] \\ \Delta\boldsymbol{q}[t_k] \end{bmatrix}. \tag{8}$$

Differently from transmission systems in which the terms $\boldsymbol{J}_{pv}[t_k]$ and $\boldsymbol{J}_{q\vartheta}[t_k]$ are assumed negligible compared to $\boldsymbol{J}_{p\vartheta}[t_k]$ and $\boldsymbol{J}_{qv}[t_k]$ because of the high reactance over resistance ratio (*X/R*), in DNs and μgs, the network lines present a lower *X/R* ratio [14]. Thus, we consider (8) to determine the effects on voltage levels of active and reactive power variation at the PCC because an effective decoupling of the effects of active and reactive power variations on voltage magnitudes and angles is not possible.

Concerning the proposed control strategy, it operates only if the voltage at the DER PCC approaches the operational limits. We define two limit droop areas as depicted in Fig. 1,

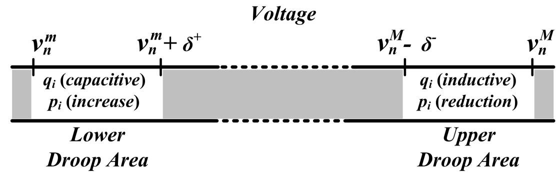

Figure 1. DERs droop thresholds.

respectively large δ^- and δ^+ and placed within the allowed voltage interval. If the voltage level at a generic bus n connected to such a resource reaches the droop area, such as the Upper Droop Area (UDA), the controller acts defining the desired voltage recovery amount, necessary to maintain voltage levels within operational limits, as in (9), depending on the resource available at bus n:

$$\Delta v_n^*[t_k] = v_n[t_k] - \left(v_n^M - \delta^-\right). \tag{9}$$

We define $\Delta\boldsymbol{v}^*[t_k]$ and $\Delta\boldsymbol{\vartheta}^*[t_k]$ as the vectors representing the desired voltage and angle variations at the μg buses for a given operating point. Taking into account the equality constraint to obtain the control action, we have:

$$\boldsymbol{J}_q^{eq}[t_k]\,\Delta\,\boldsymbol{v}^*[t_k] = \Delta\,\boldsymbol{q}[t_k] \tag{10}$$

where:

$$\boldsymbol{J}_q^{eq}[t_k] = \boldsymbol{J}_{qv}[t_k] - \boldsymbol{J}_{q\vartheta}[t_k]\left(\boldsymbol{J}_{p\vartheta}[t_k]\right)^{-1}\boldsymbol{J}_{pv}[t_k] \tag{11}$$

and we assume that $\boldsymbol{J}_{p\vartheta}[t_k]$ is not singular [15].

We determine the reactive power support shared among the DERs connected to the respective buses for which a voltage variation is required using (10), taking into account the DER costs defined in the following Section. If the overall available reactive power support for such a bus $n \in \mathscr{N}$ is less than required, we update the sensitivity factors for the new working point and compute an active power curtailment for the resources connected to that bus:

$$\Delta\boldsymbol{p}^*[t_k] = \boldsymbol{J}_p^{eq}[t_k]\,\Delta\,\boldsymbol{v}^{**}[t_k] \tag{12}$$

where:

$$\boldsymbol{J}_p^{eq}[t_k] = \boldsymbol{J}_{pv}[t_k] - \boldsymbol{J}_{p\vartheta}[t_k]\left(\boldsymbol{J}_{q\vartheta}[t_k]\right)^{-1}\boldsymbol{J}_{qv}[t_k]. \tag{13}$$

The procedure concerning the Lower Droop Area (LDA) violation is not described here due to space limitation, but it is almost symmetrical to the one illustrated for the UDA. The main difference is that in the this case we do not implement any active power increase action from renewable energy based DERs to boost the voltage level because we consider them dispatched at their maximum active power production.

III. Optimization Problem Formulation

To implement the optimization problem formulation, we assume that the μg is managed by a single entity, which sells the internal DER power in order to maximize the benefits for the μg customers. We manage renewable energy resources dispatching all their available power, in order to maximize the environmental benefits connected to them. To maximize active power production from such a renewable resource, we implement a reactive power support computation as the first step to face voltage limit violations. Thus, an active power curtailemnt takes place only if reactive power support is not enough to maintain the voltage level within the allowed limits.

The objective function of the optimization procedure is to minimize production costs within the μg. In the GCM, we consider Locational Marginal Prices (LMPs) from the day ahead market for the main reference bus.

We integrate DRRs taking into account the chronological limitations of typical demand response programs. Considering the 24 hours snapshot optimization period integrating the voltage control approach, we define a subset of the period for the DRR modulation window ($\mathscr{T}_c \subset \mathscr{T}$) and a different subset $\mathscr{T}_r \subset \mathscr{T}$ for the recovery action. We define the objective function as the cost minimization function in (14), where $c_0\big(p_0\,[t_k]\big)$ is the LMP related to the power $p_0\,[t_k]$ acquired from the external main grid and $c_s\big(p_s\,[t_k]\big)$ is the production cost of DGs and ESSs.

$$\min_{p_s} \sum_{t_k \in \mathscr{T}} \Big(c_0\big(p_0\,[t_k]\big) + \sum_{s \in \mathscr{S}} c_s\big(p_s\,[t_k]\big)\Big). \tag{14}$$

We include in the optimization procedure the constraints in (6) and (15) to (25) $\forall s \in \mathscr{S}, \forall n \in \mathscr{N}, \forall t_k \in \mathscr{T}$ and $\forall l \in \mathscr{L}$:

- power factor specifications:

$$\zeta^m \le \zeta_s = \frac{p_s\,[t_k]}{\sqrt{p_s^2\,[t_k] + q_s^2\,[t_k]}} \le 1.0 \tag{15}$$

- generator ramping limits:

$$-\Delta\, p_s^m \le \Delta\, p_s\,[t_k] \le \Delta\, p_s^M \tag{16}$$

- generator capability curves:

$$q_s^m\,[t_k] \le q_s\,[t_k] \le q_s^M\,[t_k] \tag{17}$$

$$p_s^m\,[t_k] \le p_s\,[t_k] \le p_s^M\,[t_k] \tag{18}$$

- energy storage system constraints:

$$\varepsilon_s^m\,[t_k] \le \varepsilon_s\,[t_k] \le \varepsilon_s^M\,[t_k] \tag{19}$$

$$\Delta p_s^m\,[t_k] \le \Delta p_s\,[t_k] \le \Delta p_s^M\,[t_k] \tag{20}$$

$$0 \le u^c\,[t_k] + u^d\,[t_k] \le 1 \qquad u^c\,[t_k]\,, u^d\,[t_k] \in \{0,1\} \tag{21}$$

- demand response resources constraints:

$$\sum_{\substack{r \in \mathscr{R} \\ t_k \in \mathscr{T}_c}} \Delta\, p_r\,[t_k]\;\Delta\, t_k \le \sum_{\substack{r \in \mathscr{R} \\ t_k \in \mathscr{T}_r}} \rho_r\, p_r\,[t_k]\;\Delta\, t_k. \tag{22}$$

$$\sum_{\substack{r \in \mathscr{R} \\ t_k \in \mathscr{T}_c}} \Delta\, p_r\,[t_k]\;\Delta\, t_k \ge \sum_{\substack{r \in \mathscr{R} \\ t_k \in \mathscr{T}_r}} \Delta\, p_r\,[t_k]\;\Delta\, t_k \tag{23}$$

$$\sum_{\substack{r \in \mathscr{R} \\ t_k \in \mathscr{T}_c}} c_r\big(p_r\,[t_k]\big) \ge \sum_{\substack{r \in \mathscr{R} \\ t_k \in \mathscr{T}_r}} c_r\big(p_r\,[t_k]\big). \tag{24}$$

- line limits:

$$a_l\,[t_k] \le a_l^M\,[t_k] \tag{25}$$

We take into account the ramping requirements related to generators in (16), while capability curve limits are considered in (17) and (18). ESS constraints take into account storage capacity limits (19), charging/discharging rates (20) and charging/discharging ($u^c\,[t_k]/u^d\,[t_k]$) status (21) within the analysis period. Concerning DRRs, ρ_r represents the percentage of the DRR actual power available to demand response (22), while $\Delta\, p_r\,[t_k]$ and $c_r\big(p_r\,[t_k]\big)$ respectively represent the power variation (23) and the controllable load cost (24) during the modulation window / recovery action. Finally, $a_l\,[t_k]$ in (25) represents the apparent power flowing through each line l, necessary to take into account thermal limits.

In the IOM it could be possible to size the μg in order to match only critical loads. Indeed, DGs and ESSs could not be capable to satisfy all the internal loads during this working mode. Thus, we consider the interval of the DRR participation to the resource mix to be dictated by the constraints related to the other generators in the μg, such as their availability and ratings. The proposed approach allows the recovery of the curtailed energy only if there is such a time slot in which a generation surplus takes place and the ESSs within the network are at their maximum State of Charge (SoC).

Concerning the objective function to run the optimization procedure in the IOM case, we consider a particular case of (14) in which the term concerning the main grid power is equal to zero because of the islanded condition of the μg. Thus, the objective function finalized to minimize the production cost from the internal resources and we consider explicitly the constraints (6) and (15) to (26), with $\mathscr{D} = \{d : n = 0,1,2,...,D\}$ representing the set of loads that do not participate to the demand response control support:

$$\sum_{\substack{s \in \mathscr{S} \\ t_k \in \mathscr{T}}} p_s\,[t_k] + \sum_{\substack{r \in \mathscr{R} \\ t_k \in \mathscr{T}_c}} p_r\,[t_k] - \sum_{\substack{r \in \mathscr{R} \\ t_k \in \mathscr{T}_r}} p_r\,[t_k] = \sum_{\substack{d \in \mathscr{D} \\ t_k \in \mathscr{T}}} p_d\,[t_k]\,. \tag{26}$$

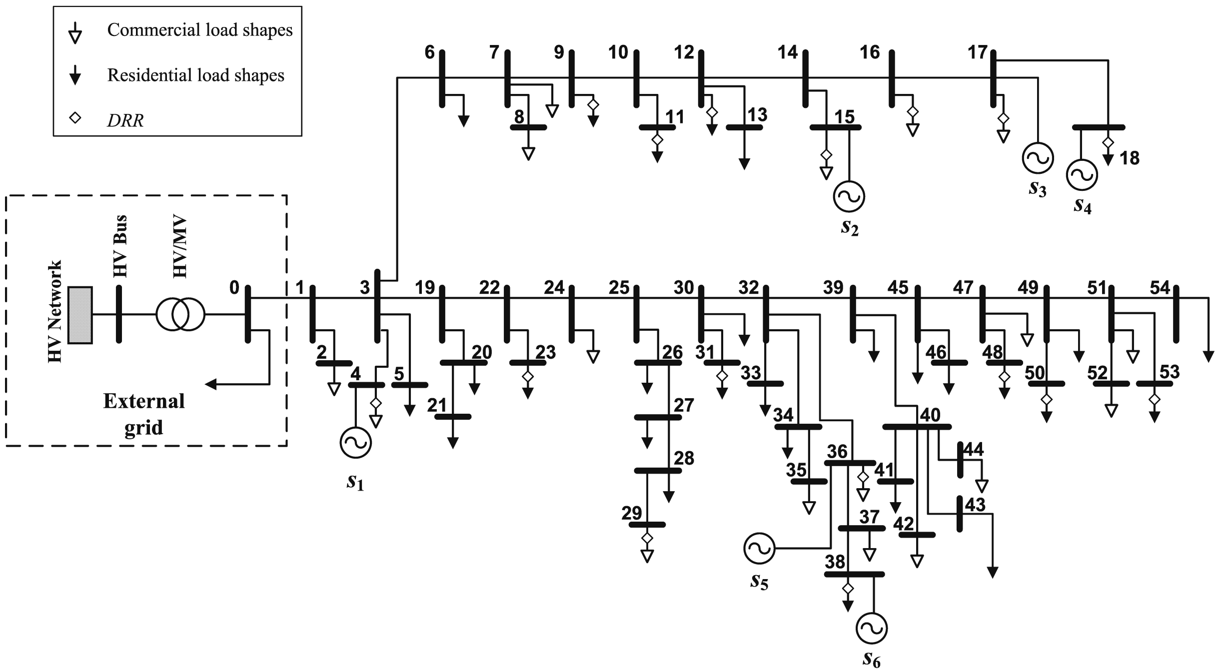

Figure 2. Test system representation.

IV. Simulation Framework and Results

In order to show the effectiveness of the proposed approach, we furnish representative studies from the extensive testing of the simulation approach we performed by running the test model with computed states every 10 minutes, in order to assure the settlement of the state changes. We base our simulations on the modified test μg depicted in Fig. 2. It represents a medium voltage radial DN [16] operated at a nominal voltage of 12kV. Compared to the reference network, we modify the peak power of a few buses as indicated in Table II [11].

TABLE II. Modified Peak Loads

bus no.	p [MVA]	bus no.	p [MVA]
39	0.130	50	0.058
45	0.234	52	0.131
47	0.296	53	0.261
49	0.145	54	0.315

We integrate into the system two microturbine (μT) Combined Heat and Power (CHP) plants, three PhotoVoltaic (PV) systems and an ESS, with their characteristics given in Table III. We remove the capacitor banks contained in the reference network to show the DERs control capabilities related to the proposed approach.

We assume the CHPs to have a modular structure and to be represented by a μT system capable to offer services such as load following control with high-level efficiencies [17]. We consider each CHP composed by five systems with rated power of 200 kVA each one and a central controller capable to coordinate the single units in order to guarantee high-level efficiencies at partial load and satisfying ramping rates to validate the snapshot analysis assumption.

TABLE III. Integrated DERs

s	type	bus no.	p [MVW]
1	μT	4	1
2	*PV*	15	0.5
3	*PV*	17	1
4	*PV*	18	1.8
5	*ESS*	36	1
6	μT	38	1

We consider each μT system to produce at least 200 kW power in the GCM in order to produce heating and/or cooling energy for the μg heating district needs. This assumption is related to the fact that the thermal model is beyond the scope of the paper, thus we only mention that excess power could be used for thermal needs or thermal storage.

We adopt a battery based ESS model characterized by 1 MW peak power rating and energy storage capacity of 3 MWh, taking into account real data from commercial products [18]. To complete the list of the available controllable resources, we show in Table IV the list of loads considered as DRRs.

Concerning the external reference bus LMPs, we simply assume that such a price signal is available since in a competitive environment the DG entities must have the reference pricing against which to compete.

We make use of real PV power profiles for winter ($\mathscr{W}$) and summer ($\mathscr{E}$). Within our analysis, we consider two days per season, a cloudy day and a sunny day. We consider load shapes defined as typical residential and commercial

TABLE IV. INTEGRATED DRRS

r	bus no.	r	bus no.
1	4	9	23
2	9	10	29
3	11	11	31
4	12	12	36
5	15	13	38
6	16	14	48
7	17	15	50
8	18	16	53

customers weekday (*wd*) and weekend (*we*) patterns, as in Fig. 3 [19]. The assumption to have only a defined residential or commercial profile at a given node, even if representing an hypotetical assumption on a MV network, allows us to obtain a differentiation among the loads located at different nodes in order to analyze a more general network test case. We show representative results for both the GCM and the IOM for the worst situation concerning voltage control, a $\mathscr{E}$ sunny *we* day.

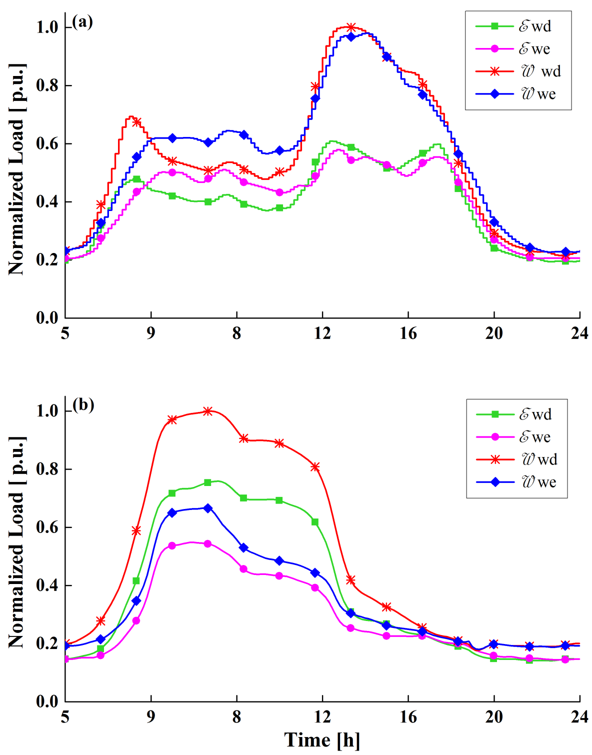

Figure 3. Load shapes - (a) GCM - (b) IOM.

We run the optimization algorithm containing the voltage control method in order to optimize the production costs for both the GCM and IOM, obtaining the resource mix shown in Fig. 4, in which it is worth to note the different scheduling of s_1, s_5 and s_6, due to the absence, in the IOM, of the main grid connection. The optimization approach reaches the objective of voltage control for the interest buses as depicted in Fig. 5.

It is worth to note that the violations of voltage limits

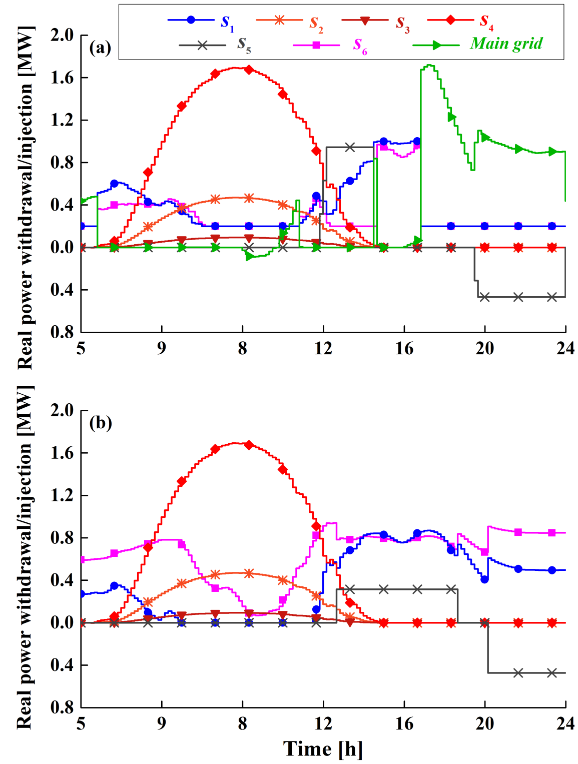

Figure 4. Active power - (a) GCM - (b) IOM.

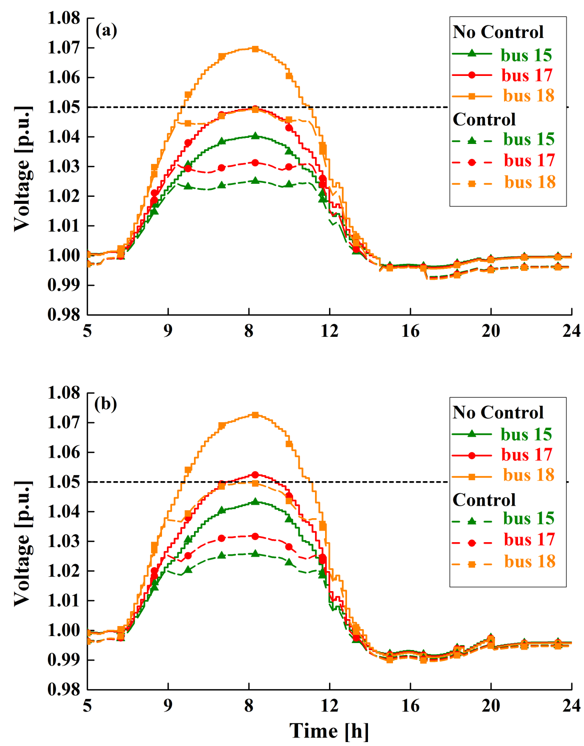

Figure 5. Voltage profiles - (a) GCM - (b) IOM.

occurring in both cases without an appropriate control strategy are well managed by the proposed solution. In particular, in the IOM working mode, both the generators connected to the buses affected by voltage limits infringement give their contribution to the control action. Voltage is maintained within operational limits by local reactive power support and without any active power curtailment. Thus, no opportunity cost is involved by the proposed approach.

In Table V, we give information concerning total costs and reactive power support obtained as part of the performed testing phase. In particular, we introduce the parameter Reactive Energy (RE), that gives the idea of the overall reactive power contribution over time during the 24 hours based simulation period. It is worth to note that in the case of clouds, e.g. for the GCM optimization, the total operation cost is higher than in the sunny case, because of the reduced contribution by PVs. For the IOM, we show representative results concerning the same days as in the GCM case, resultant in a higher reactive power support contribution compared to the GCM, mainly due to the absence of the main grid reference bus connection.

TABLE V. GCM AND IOM COSTS AND REACTIVE POWER SUPPORT.

Season		**Total Cost [k$]**		**Total *q***		**Total RE**	
Summer		GCM	IOM	GCM	IOM	GCM	IOM
sunny	*wd*	6.28	6.68	15.88	19.93	5.29	6.64
	we	5.80	5.88	16.56	20.92	5.52	6.98
cloudy	*wd*	6.45	6.78	15.25	18.86	5.09	6.29
	we	5.99	5.98	15.81	19.11	5.27	6.37

Concerning the DRRs, such a least effective result in terms of providing voltage control is in line with the low sensitivity associated with such resources. Thus, we present the concept of DRRs incrementing the load to implement a voltage reduction, as introduced in [10], as a least effective resource to use within the proposed approach. Indeed, from the simulation testing activities, we gained the confirmation of a small impact of this control component on voltage profiles.

V. CONCLUSIONS

In this paper, we presented the development of a DER based voltage control technique for μg applications, capable to avoid voltage limits infringement at the PCC between the DER and the μg feeder. We modeled a sensitivity factors based control action and we incorporated it into an optimization framework finalized to reduce the overall energy costs for the μg customers. We run the optimization approach for both the GCM and the IOM, proving its cost effective characteristics and the possibility to implement voltage control actions overcoming, at least in part, the utilization of traditional voltage control devices (e.g. on-load tap changers and capacitor banks). We pointed out the necessity to employ flexible generators to guarantee load following capabilities and spark-spread characteristics, obtaining the machine scheduling as a compromise between technical and economic constraints.

The proposed approach represents an effective tool for both planning and operational control of DERs, trying to maximize the utilization of renewable resources.

REFERENCES

[1] T. L. Vandoorn, B. Meersman, J. D. M. De Kooning and L. Vandevelde, ”Transition from islanded to grid-connected mode of microgrids with voltage-based droop control”, *IEEE Trans. Power Syst.*, vol 28, no. 3, pp. 2545-2553, 2013.

[2] A.H. Etemadi, E. J. Davison and R. Iravani, ”A decentralized robust control strategy for multi-DER microgrids - part I: fundamental concepts”, *IEEE Trans. Power Deliv.*, vol. 27, no. 4, pp. 1843-1853, 2012.

[3] M. S. P. Carvalho, P. F. Correia and Lus A. F. M. Ferreira, ”Distributed Reactive Power Generation Control for Voltage Rise Mitigation in Distribution Networks”, IEEE Trans. Power Syst., vol. 23, no. 2, pp. 766-772, 2008.

[4] A. Keane, L. F. Ochoa, E. Vittal, C. J. Dent and G. P. Harrison, ”Enhanced Utilization of Voltage Control Resources With Distributed Generation”, *IEEE Trans. Power Syst.*, vol. 26, no. 1, pp. 252-260, 2011.

[5] H. Li, F. Li, Y. Xu, D. T. Rizy and S. Adhikari, ”Autonomous and adaptive voltage control using multiple distributed energy resources”, *IEEE Trans. on Power Syst.*, vol. 28, no. 2, pp. 718-730, 2013.

[6] Y. P. Agalgaonkar, B. C. Pal and R. A. Jabr, ”Distribution voltage control considering the impact of PV generation on tap changers and autonomous regulators”, *IEEE Trans. on Power Syst.*,vol. 29, no. 1, pp. 182-192, 2014.

[7] P. Jahangiri and D. C. Aliprantis, ”Distributed Volt/VAr control by PV inverters”, *IEEE Trans. Power Syst.*, vol. 28, no. 3, pp. 3429-3439, 2013.

[8] M. Falahi, K. Butler-Purry and M. Ehsani, ”Dynamic reactive power control of islanded microgrids”, *IEEE Trans. Power Syst.*, vol. 28, no. 4, pp. 3649-3657, 2013.

[9] V. Calderaro, G. Conio, V. Galdi, G. Massa and A. Piccolo, ”Optimal decentralized voltage control for distribution systems with inverter based distributed generators”, *IEEE Trans. Power Syst.*, vol. 29, no. 1, pp. 230-241, 2014.

[10] T. L. Vandoorn, B. Renders, L. Degroote, B. Meersman and L. Vandevelde, ”Active load control in islanded microgrids based on the grid voltage”, *IEEE Trans. Smart Grid*, vol. 2, no. 1, pp. 139-151, 2011.

[11] G. Massa, G. Gross, V. Galdi, A. Piccolo, ”Dispersed voltage control in microgrids”, *IEEE Trans. Power Syst.*, accepted for publication on a future issue of the journal, DOI: 10.1109/TPWRS.2015.2503393, pp. 1-11, 2015.

[12] R. A. Walling, R. Saint, R. C. Dugan, J. Burke and L. A. Kojovic, ”Summary of distributed resources impact on power delivery systems”, *IEEE Trans. Power Del.*, vol. 23, no. 3, pp. 1636-1644, 2008.

[13] Y. Degeilh, J. Descloux and G. Gross, ”Simulation of energy storage in a system with integrated wind resources”, in *Proc. 17th Power System Comp. Conf.*, pp. 1-7, 2011.

[14] H. Bevrani and S. Shokoohi, ”An intelligent droop control for simultaneous voltage and frequency regulation in islanded microgrids”, *IEEE Trans. Smart Grid*, vol. 4, no. 3, pp. 1505-1513, 2013.

[15] A. B. Almeida, E. V. De Lorenci, R. C. Leme, A. C. Zambroni de Souza, B. I. Lima Lopes and K. Lo, ”Probabilistic voltage assessment considering renewable sources with the help of the PV and QV curves”, *IET Renew. Power Gener.*, vol. 7, no. 5, pp. 521-530, 2013.

[16] M. Farivar, R. Neal, C. Clarke and S. Low, ”Optimal inverter VAr control in distribution systems with high PV penetration”, in *Proc. of IEEE Power and Energy Society General Meeting*, San Diego, pp. 1-7, 2012.

[17] Capstone Turbine Corporation, ”Capstone C1000 Microturbine Systems technical reference”, available online: http://www.regattasp.com/files/410072A-C1000-TR.pdf, pp. 49-54, 85-93, 2009.

[18] ABB, ”Energy storage modules (ESM) Up to 4 MW”, available online: http://www05.abb.com/global/scot/scot235.nsf/veritydisplay/f09413974e2f041cc12579e3004fa562/file/energy-storage-modules-brochure-rev-e.pdf, pp. 1-19, 2012.

[19] Elexon, Profiling samples and candidate selection, available online: http://www.elexon.co.uk/reference/technical-operations/profiling/, pp. 1-16, 2013.